

# Instantaneous Frequency in Power Systems using the Teager-Kaiser Energy Operator

Angel Vaca, *IEEE Student Member*, Joan Gutiérrez-Florensa, *IEEE Student Member*, and Federico Milano, *IEEE Fellow*

**Abstract**—This paper develops an instantaneous-frequency (IF) local estimator calculated with the complex Teager–Kaiser energy operator (CTKEO) and the dynamic-signal identity. The contribution is a novel IF expression that makes the envelope-curvature terms explicit, thus correcting the bias that affects conventional estimators used in power systems. The estimator aligns with complex-frequency (CF) kinematics and admits a geometric interpretation (curvature/torsion) without phase unwrapping. Simulations and data-driven examples demonstrate the accuracy of the proposed approach.

**Index Terms**—Teager-Kaiser Energy Operator (TKEO), instantaneous frequency, complex frequency, differential geometry

## I. INTRODUCTION

The estimation of instantaneous frequency (IF) remains a central problem in signal analysis, fundamental to characterizing nonstationary and time-varying phenomena [1]–[3]. This problem has been addressed by a range of methods available in the literature, including phase-locked loop (PLL) [4], discrete Fourier transform [5], Kalman filters [6], least squares [7], adaptive notch filters [8], among others. The diversity of available techniques suggests that none is optimal, and the suitability of each approach depends on the particular application, thereby leaving scope for further research.

Recent theoretical advances have reframed the notion of frequency through complex frequency, that expresses the differential behavior of electrical variables as complex power and voltages at network buses [9], and through a differential-geometry framework, that interprets frequency as the “curvature” of voltage trajectories in multidimensional space [10], [11], and provides a unified description of time- and phasor-domain dynamics [12].

In this work, we consider a different approach to estimate IF based on the Teager-Kaiser Energy Operator (TKEO). This operator features locality, physical interpretability, and computational simplicity. Introduced as a nonlinear measure of the energy required to generate a signal [13], TKEO relates instantaneous energy to temporal derivatives, enabling direct access to magnitude and frequency variations without explicit phase reconstruction [14], [15]. Applications of TKEO span speech, biomedical, and mechanical systems, where it demonstrates robustness under strong nonstationarity and noise [16], [17]. In power systems, the operator has been utilized for

The authors are with the School of Electrical and Electronic Engineering, University College Dublin, Belfield Campus, D04V1W8, Ireland. e-mails: angel.vaca1@ucdconnect.ie, joan.gutierrezflorensa1@ucdconnect.ie, federico.milano@ucd.ie

This work is supported by the Science Foundation Ireland (SFI) by funding the authors under NexSys project, Grant No. 21/SPP/3756.

real-time tracking of electromechanical oscillations and local frequency dynamics from phasor measurements [18].

Existing TKEO formulations rely on narrow-band assumptions and slowly varying envelopes, limiting their accuracy during transients or unbalanced operation. Moreover, numerical differentiation introduces noise sensitivity, and scalar operators that limit the capture of the coupled magnitude–phase behavior of complex phasors [19].

This paper extends the TKEO to complex signals and derives a formulation that unifies nonlinear energy and geometric interpretations. The resulting proposed formula yields exact instantaneous frequency estimation directly from local derivatives, bridging classical energy demodulation with modern curvature-based models of power-system dynamics.

The remainder of this paper is organized as follows. Section II introduces the proposed frequency estimation based on CTKEO. Section III presents relevant analytical and numerical examples that illustrate the findings of the previous section. Section IV examines the behavior of the proposed method in realistic simulation and real-data case scenarios. Finally, conclusions are provided in Section V.

## NOTATION

Scalar quantities are represented with italic font, e.g.,  $a$  or  $A$ ; vectors with bold lower case, e.g.,  $a$ ; and complex numbers with a bar over it, e.g.,  $\bar{a}$ . The magnitude of a complex number  $\bar{a}$  is denoted with  $|\bar{a}|$ , its complex conjugate with  $\bar{a}^*$ , and the time derivative of a quantity  $a$  with  $a'$ . Unless indicated otherwise, quantities are assumed to be time-dependent.

## II. COMPLEX TEAGER–KAISER ENERGY OPERATOR

The conventional continuous-time Teager–Kaiser energy operator for real signals is defined as:

$$\Psi_{\mathbb{R}}(x) = (x')^2 - x x''. \quad (1)$$

This quantity measures the instantaneous “frequency-weighted energy” of  $x$ . In discrete time, for a time series  $x_1, x_2, \dots, x_N$ , it takes the form:

$$\Psi_{\mathbb{R}}(x_n) = (x_n)^2 - x_{n-1} x_{n+1}, \quad n \in \{2, \dots, N-1\}. \quad (2)$$

An established application of the Teager–Kaiser operator is the Energy Separation Algorithm (ESA), originally developed for the demodulation of amplitude–frequency modulated (AM–FM) signals [14], [20]. Consider a real AM–FM component:

$$x = a \cos(\phi) = a \cos\left(\int_0^t \omega d\tau + \phi(0)\right), \quad (3)$$

where both  $a$  and  $\omega = \phi'$  vary slowly relative to the carrier. When the real TKEO defined in (1) is applied to such a signal, it yields:

$$\Psi_{\mathbb{R}}(x) \approx a^2 \omega^2, \quad (4)$$

which represents an instantaneous, frequency-weighted energy proportional to the square of both amplitude and angular frequency. This approximation holds under the so-called “narrow-band” or “slow-envelope” condition, and is verified in [13] and others.

Applying the operator to the time derivative of the signal produces

$$\Psi_{\mathbb{R}}(x') \approx a^2 \omega^4, \quad (5)$$

and combining (4) and (5) eliminates the amplitude term, giving the classical ESA relations:

$$a \approx \frac{\Psi_{\mathbb{R}}(x)}{\sqrt{\Psi_{\mathbb{R}}(x')}}, \quad \omega \approx \sqrt{\frac{\Psi_{\mathbb{R}}(x')}{\Psi_{\mathbb{R}}(x)}} \quad (6)$$

Equations (6) provide instantaneous estimates of amplitude and frequency, respectively.

Despite its simplicity, the ESA accuracy degrades when envelope or frequency variations are fast, the signal cannot be modeled directly as a cosine function, or when multiple components overlap — conditions often observed in power system dynamics [21].

#### A. Extension to complex signals

While ESA is formulated for real, narrow-band signals, voltage and current phasors in power systems are inherently complex-valued and exhibit significant magnitude variations during transient operation. To address these limitations, the TKEO can be generalized to complex signals by employing the symmetric bilinear form:

$$\Psi_{\mathbb{B}}(\bar{x}, \bar{y}) = \frac{1}{2}(\bar{x}'^* \bar{y}' + \bar{x}' \bar{y}'^*) \quad (7)$$

$$- \frac{1}{4}(\bar{x} \bar{y}''^* + \bar{x}^* \bar{y}'' + \bar{y} \bar{x}''^* + \bar{y}^* \bar{x}''). \quad (8)$$

In the special case where  $x \equiv y$ , this reduces to:

$$\Psi_{\mathbb{C}}(\bar{x}) \equiv \Psi_{\mathbb{B}}(\bar{x}, \bar{x}) = |\bar{x}'|^2 - \text{Re}(\bar{x} \bar{x}''^*). \quad (9)$$

The operator  $\Psi_{\mathbb{C}}(\bar{x})$  is real, additive on Cartesian components, and invariant to constant phase shifts. It therefore extends the real TKEO to complex trajectories without imposing narrow-band or slow-envelope constraints.

Alternatively, from (8), expressing  $\bar{x}$  in terms of its real and imaginary parts, one can easily verify that:

$$\Psi_{\mathbb{C}}(\bar{x}) \equiv \Psi_{\mathbb{B}}(\bar{x}, \bar{x}) = \Psi_{\mathbb{R}}(\text{Re}(\bar{x})) + \Psi_{\mathbb{R}}(\text{Im}(\bar{x})), \quad (10)$$

as proposed in [22], [23]. This relation allows us to use the identity in (2) to calculate  $\Psi_{\mathbb{C}}$  for discrete time.

#### B. TKEO in terms of complex frequency

Let  $\bar{x} = |\bar{x}|e^{j\phi}$  denote an analytic AM-FM signal. We recall the complex frequency definition — see the Appendix:

$$\bar{\eta} = \frac{\bar{x}'}{\bar{x}} = \frac{|\bar{x}|'}{|\bar{x}|} + j\phi' = \rho + j\omega, \quad (11)$$

where  $\rho = |\bar{x}'|/|\bar{x}|$  and  $\omega = \phi'$  are the instantaneous magnitude and angular rates, respectively. Using  $\bar{x}' = \bar{\eta}\bar{x}$  and  $\bar{x}'' = (\bar{\eta}' + \bar{\eta}^2)\bar{x}$ , substitution into (9) yields:

$$\Psi_{\mathbb{C}}(\bar{x}) = |\bar{x}|^2(|\bar{\eta}|^2 - \text{Re}(\bar{\eta}'^* + \bar{\eta}^{*2})). \quad (12)$$

Expanding  $\bar{\eta} = \rho + j\omega$  gives  $|\bar{\eta}|^2 = \rho^2 + \omega^2$  and  $\text{Re}(\bar{\eta}'^* + \bar{\eta}^{*2}) = \rho' + \rho^2 - \omega^2$ , leading to the formula:

$$\Psi_{\mathbb{C}}(\bar{x}) = |\bar{x}|^2(2\omega^2 - \rho'). \quad (13)$$

This result generalizes the ESA principle without approximations, and also separates the local energy into two interpretable parts: the rotational component  $(2|\bar{x}|^2\omega^2)$ , and a translation term  $(-|\bar{x}|^2\rho')$  that accounts for magnitude variations.

#### C. Instantaneous frequency of the voltage

Let us now assume that two coordinates can describe the voltage at a node of a three-phase system, say  $(v_{\alpha}, v_{\beta})$ . As demonstrated in [24], this is always possible in case torsion is zero. This assumption is not particularly restrictive, as torsion is not zero only under very special operating conditions, e.g., during a fault or with unbalanced harmonics, which are not commonly encountered in transmission and distribution systems. Typical balanced, unbalanced and non-sinusoidal scenarios have in fact zero torsion. Moreover, if in addition to zero torsion, the zero sequence is also null,  $(v_{\alpha}, v_{\beta})$  corresponds to the coordinates of the conventional Clarke transform [24]. Then, as detailed in the Appendix, we can define a complex voltage signal as:

$$\bar{v} = v_{\alpha} + jv_{\beta} = |\bar{v}|e^{j\theta}. \quad (14)$$

Assuming  $\bar{x} = \bar{v}$  and  $\phi = \theta$ , and substituting  $\rho = |\bar{x}'|/|\bar{x}|$  into (13) yield:

$$\begin{aligned} \frac{\Psi_{\mathbb{C}}(\bar{v})}{|\bar{v}|^2} &= 2\omega^2 - \rho' \\ &= 2\omega^2 + \left(\frac{|\bar{v}'|}{|\bar{v}|}\right)^2 - \frac{|\bar{v}''|}{|\bar{v}|}. \end{aligned} \quad (15)$$

Solving for  $\omega$  yields the proposed expression for the instantaneous frequency:

$$\omega_{\text{TV}} = \sqrt{\frac{1}{2} \left[ \frac{\Psi_{\mathbb{C}}(\bar{v})}{|\bar{v}|^2} - \left( \frac{|\bar{v}'|}{|\bar{v}|} \right)^2 + \frac{|\bar{v}''|}{|\bar{v}|} \right]} \quad (16)$$

The subscript TV indicates that expression (16) is obtained considering  $|\bar{v}|$  as a time-varying quantity. Unlike the approximate ESA results, equation (16) constitutes a bias-corrected instantaneous frequency estimator that remains exact even under rapid magnitude variations.

If  $|\bar{v}|$  is constant or shows slow variations, this expression reduces to  $\Psi_{\mathbb{C}}(\bar{v}) = 2|\bar{v}|^2\omega^2$ , and the instantaneous frequency estimator becomes:

$$\omega_{\text{TI}} = \frac{1}{\sqrt{2}} \sqrt{\frac{\Psi_{\mathbb{C}}(\bar{v})}{|\bar{v}|^2}} \quad (17)$$

where the subscript indicates that expression (17) is obtained considering  $|\bar{v}|$  as a time-invariant quantity.

The case study discussed in Section IV illustrates the accuracy of the expression (16) as well as of (17).

#### D. Geometric and physical interpretation in power systems

The complex TKEO identities derived above can be understood through the lens of the complex-frequency and geometric frameworks. The quantity  $\eta = \rho + j\omega$  describes the instantaneous evolution of a phasor in the complex plane:  $\rho$  represents the logarithmic rate of change of its magnitude, and  $\omega$  the angular velocity of its rotation. In this setting, the two terms in  $\Psi_{\mathbb{C}}(\bar{x}) = |\bar{x}|^2(2\omega^2 - \rho')$  acquire clear physical meaning:  $2|\bar{x}|^2\omega^2$  corresponds to rotational (phase) energy, while  $-|\bar{x}|^2\rho'$  accounts for the curvature of the envelope, capturing magnitude-driven effects.

From a geometric viewpoint,  $\omega$  measures the curvature of the voltage trajectory, and  $\omega'$  quantifies its rate of change. This separation mirrors recent results showing that geometric frequency admits a decomposition into rotational and distortion components via the Lagrange derivative, reinforcing the interpretation of the Teager–Kaiser operator as a strictly local estimator of rotational dynamics, as in [25].

This interpretation is consistent with the complex-frequency differential  $\bar{v}' = (\rho + j\omega)\bar{v}$ , which governs the local kinematics of voltage phasors. Consequently, the CTKEO links nonlinear energy analysis with the intrinsic geometry of phasor motion:  $\omega$  and  $\omega'$  correspond respectively to the curvature and curvature rate of the trajectory. Moreover, unlike non-local geometric frequency concepts based on trajectory closure or circulation [26], the proposed estimator remains entirely local in time, relying exclusively on derivatives of the measured signal.

### III. ILLUSTRATIVE EXAMPLES

In this section, we present an analytical appraisal to illustrate the behavior of the proposed estimator under relevant conditions. We assume that the three-phase voltage is defined in the complex  $\alpha\beta$  plane — e.g., torsion is zero —, as follows:

$$\begin{aligned}\bar{v} &= v_{\alpha} + jv_{\beta} \\ &= |v_{\alpha}| \cos \theta + j|v_{\beta}| \sin \theta.\end{aligned}\quad (18)$$

In the remainder of this section, we consider two scenarios: (i) balanced sinusoidal voltage, and (ii) unbalanced nonsinusoidal voltage.

#### A. Balanced sinusoidal voltage

Under perfectly balanced and sinusoidal conditions, amplitudes are constant and equal to  $|v_{\alpha}| = |v_{\beta}| = |\bar{v}|$ , and  $\theta = \omega_0 t + \xi$ , where  $\omega_0$  is the fundamental angular frequency of the sinusoid and  $\xi$  is the initial angular shift. Then, the following identities hold:

$$\begin{aligned}\bar{v} &= |\bar{v}| e^{j(\omega_0 t + \phi)}, \\ \Rightarrow \bar{v}' &= j\omega_0 \bar{v}, \\ \Rightarrow \bar{v}'' &= -\omega_0^2 \bar{v}.\end{aligned}\quad (19)$$

Substituting these identities into (9), CTKEO is obtained:

$$\Psi_{\mathbb{C}}(\bar{v}) = |\bar{v}'|^2 - \operatorname{Re}(\bar{v} \bar{v}'^*) = 2\omega_0^2 |\bar{v}|^2, \quad (20)$$

and from (16), the instantaneous frequency is estimated as:

$$\omega_{\text{TV}} = \sqrt{\frac{1}{2} \left[ \frac{2\omega_0^2 |\bar{v}|^2}{|\bar{v}|^2} - \frac{0}{|\bar{v}|^2} + \frac{0}{|\bar{v}|} \right]} = \omega_0, \quad (21)$$

In this case, the approximation, under the constant magnitude assumption, by means of (17), coincides with this value:

$$\omega_{\text{TI}} = \frac{1}{\sqrt{2}} \sqrt{\frac{2\omega_0^2 |\bar{v}|^2}{|\bar{v}|^2}} = \omega_0. \quad (22)$$

The real signals  $v_{\alpha}$  and  $v_{\beta}$  lead to:

$$\begin{aligned}\Psi_{\mathbb{R}}(v_{\alpha}) &= \Psi_{\mathbb{R}}(v_{\beta}) = \omega_0^2 |\bar{v}|^2, \\ \Psi_{\mathbb{R}}(v'_{\alpha}) &= \Psi_{\mathbb{R}}(v'_{\beta}) = \omega_0^4 |\bar{v}|^2,\end{aligned}\quad (23)$$

where the identity  $\bar{v}''' = -j\omega_0^3 \bar{v}$  has been used. Frequency estimation by means of classic ESA relations gives:

$$\omega_{\alpha} = \sqrt{\frac{\Psi_{\mathbb{R}}(v'_{\alpha})}{\Psi_{\mathbb{R}}(v_{\alpha})}} = \omega_0; \quad \omega_{\beta} = \sqrt{\frac{\Psi_{\mathbb{R}}(v'_{\beta})}{\Psi_{\mathbb{R}}(v_{\beta})}} = \omega_0. \quad (24)$$

All results above match because: (i) the approximation used in (22) assumes  $\rho = 0$ ; and (ii) estimation by the classical approach in (24) requires that the frequency of the real term and of the imaginary term coincide and are equal to the frequency signal.

#### B. Unbalanced nonsinusoidal voltage

We consider the unbalanced case  $|v_{\alpha}| = 0.8|v_{\beta}|$  and the introduction of an harmonic of order  $h = 5$  and magnitude  $|\bar{v}_h| = 0.01|\bar{v}|$  are assessed and illustrated in the following figures. Figs. 1a and 1c show  $\omega_{\text{TV}}$  and  $\omega_{\text{TI}}$  for the former and the latter cases, respectively, while figs. 1b and 1d show  $\omega_{\alpha}$  and  $\omega_{\beta}$  correspondingly. Results are compared with the instantaneous frequency magnitude computed through the geometric definition of  $\omega_v$  given in (28) — see the Appendix. This choice is motivated by the conclusion in [27] that  $\omega_v$  closely matches the frequency estimation of a PLL.

Estimations of  $\omega_{\alpha}$  and  $\omega_{\beta}$  from the classical approach differ from  $\omega_v$  because they measure different quantities. The instantaneous frequency of voltage defines the curvature of the trajectory in the  $(v_{\alpha}, v_{\beta})$  plane and therefore requires information from both axes, whereas estimating the frequency of each component, as a real signal, ignores cross-information and only matches  $\omega_v$  under ideal sinusoidal conditions.

On the other hand,  $\omega_{\text{TV}}$  matches the  $\omega_v$  value whereas  $\omega_{\text{TI}}$  only approximates it. Under certain operation conditions, voltage can be represented by a phasor with a time-varying magnitude and rotation. The latter term is the quantity that ESA's frequency estimation measures. As in this case, the time dependency of the magnitude is not negligible,  $\omega_{\text{TI}}$  does not yield accurate results.

### IV. CASE STUDIES

In this section, the performance and practical applicability of the proposed frequency estimation,  $\omega_{\text{TV}}$ , and the approximation,  $\omega_{\text{TI}}$ , are evaluated. To this aim, two case studies are presented: (i) based on a simulated test; and (ii) based on actual measurement data.  $\Psi_{\mathbb{C}}$  is computed with the discrete

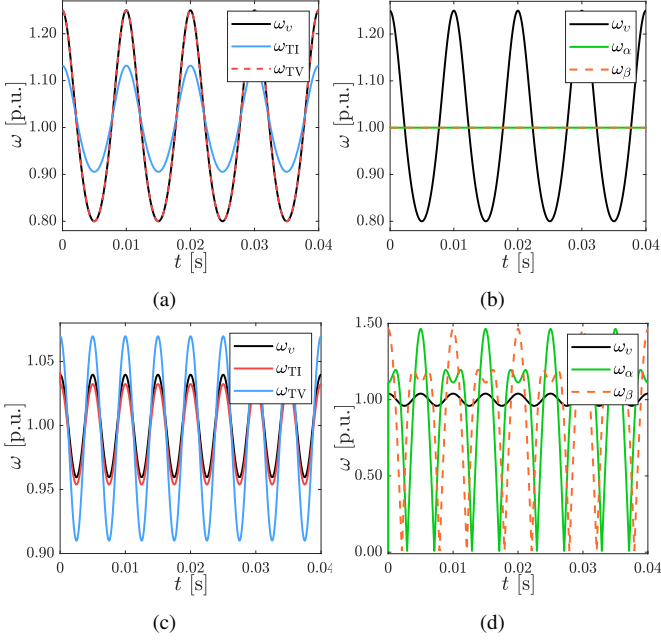


Fig. 1: Frequency estimation results under stationary conditions with: (a, b) a magnitude unbalance of  $|v_\alpha| = 0.8|v_\beta|$ ; and (c, d) the presence of a balanced harmonic of order  $h = 5$  and magnitude  $|\bar{v}_h| = 0.01|\bar{v}|$ .

expressions (2) and (10), and all the frequency estimations were passed through a discrete Butterworth filter.

#### A. EMT Simulation of IEEE 39-Bus System

In this case study, the IEEE 39-bus system, from DIgSILENT PowerFactory software tool, is assessed. The considered signal is the three-phase voltage at bus 26 following a three-phase fault at bus 4 at  $t = 0.2$  s, cleared at  $t = 0.3$  s. The tests consider two different scenarios: balanced system operation with Gaussian noise in the voltage measurement, Fig. 2a, and unbalanced operation, Fig. 2b.

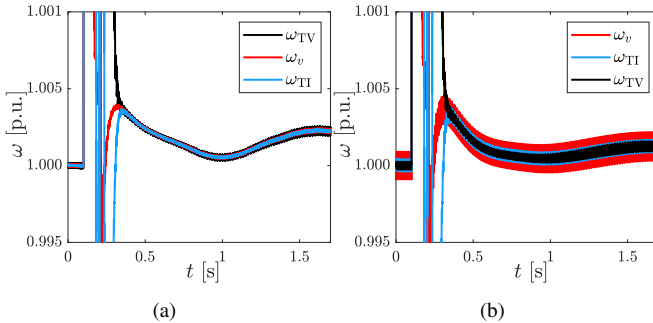


Fig. 2: Frequency results bus 26, of the IEEE 39-bus system for a secured three-phase fault under: (a) balanced conditions with Gaussian noise in the voltage; and (b) unbalanced operation.

Results under balanced conditions with noise show that estimations from the three approaches do not differ significantly. Both scenarios show that frequency estimation from  $\omega_{TI}$  and  $\omega_{TV}$  closely match because the variations in the voltage magnitude are relatively slow and small, and are

mitigated by filtering the time series. On the other hand, in the unbalanced scenario,  $\omega_{TI}$  and, especially,  $\omega_{TV}$  show lower oscillations, before and after the fault, with respect to  $\omega_v$ , as this quantity captures the imbalances as a distortion in the voltage curvature; demonstrating the accuracy of the proposed estimation methods.

#### B. Voltage Measurements at a PV Power Plant

To further assess the performance of the proposed  $\omega_{TI}$  and  $\omega_{TV}$ , we consider actual field measurements of the voltage at the point of connection to the grid of a PV power plant in Moralejo, Spain. From this data, the first requirement for an accurate computation of  $\omega_{TV}$  is to filter both  $v'$  and  $v''$  measurements, while for  $\omega_v$ , only  $v'$  is filtered.

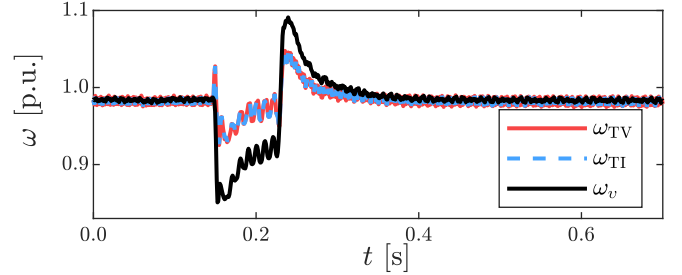


Fig. 3: Frequency estimation results from the real voltage measurements at the point of connection to the grid of a PV power plant.

Results in Fig. 3, show that both  $\omega_{TI}$  and  $\omega_{TV}$  closely match  $\omega_v$ . Although  $\omega_{TI}$  does not account for magnitude variations, the combined effect of voltage filtering and the inherently slow dynamics of  $\rho$  under realistic operating conditions makes this approximation practically equivalent to the full time-varying estimation. These results indicate that  $\omega_{TI}$  provides a close approximation of instantaneous frequency, whereas  $\omega_{TV}$  results in a more precise but also slightly more demanding, in terms of numerical computation, estimation.

In this case, the former offers an approximate yet reliable alternative that is especially attractive for real-time applications, particularly when compared with more complex approaches such as PLL-based frequency estimation. Compared with  $\omega_v$ , the proposed approach takes advantage of the robustness of TKEO and offers a frequency definition that decomposes it into different terms, the relevance of each of which can be assessed individually. The bulk of the estimation is given by  $\Psi_C(\bar{v})/|\bar{v}|^2$  whereas the voltage magnitude rate of change terms can be understood as “corrections” of the former term. These corrections determine the accuracy of the approximated expression that returns  $\omega_{TI}$ .

## V. CONCLUSIONS

This paper presents a formulation of instantaneous frequency derived from the complex TKEO. Starting from the dynamic-signal identity and applying it to power-system phasors, we obtain a precise local expression for frequency that remains valid under rapid magnitude changes and unbalances. The method aligns with complex-frequency kinematics and offers a geometric interpretation in which  $\omega$  describes the

curvature of voltage trajectories. By unifying nonlinear energy analysis and geometric frequency theory, the proposed approach provides a compact and physically interpretable tool for real-time monitoring of power system dynamics. In addition to the proposed formulation, an approximated form is introduced with significantly simpler numerical computation while retaining accuracy under realistic operating conditions for practical implementation.

## APPENDIX

Instantaneous frequency estimation through energy operators requires a framework capable of describing both magnitude and phase dynamics. This section introduces the key mathematical elements that support the derivations presented in the paper.

Let us assume the instantaneous complex voltage is:

$$\bar{v} = v_\alpha + jv_\beta = |\bar{v}|e^{j\theta} \in \mathbb{C}, \quad (25)$$

where  $v_\alpha$  and  $v_\beta$  are the components of the Clarke transform of the voltage,  $|\bar{v}| > 0$  and  $\theta$  denote the instantaneous magnitude and phase, respectively. Its first derivative,  $\bar{v}'$  can be expressed as:

$$\bar{v}' = \left( \frac{|\bar{v}|'}{|\bar{v}|} + j\theta' \right) \bar{v} \triangleq (\rho_v + j\omega_v) \bar{v} \equiv \bar{\eta}_v \bar{v}, \quad (26)$$

where:

$$\rho_v = \frac{|\bar{v}|'}{|\bar{v}|} = \frac{v_\alpha v'_\alpha + v_\beta v'_\beta}{v_\alpha^2 + v_\beta^2} \quad (27)$$

represents the *instantaneous radial frequency* or *instantaneous bandwidth*,

$$\omega_v = \theta' = \frac{v_\alpha v'_\beta + v_\beta v'_\alpha}{v_\alpha^2 + v_\beta^2} \quad (28)$$

is the *instantaneous angular frequency*, and  $\bar{\eta}_v = \rho_v + j\omega_v$  is the complex frequency.

In discrete time, for time series  $v_{\alpha,1}, v_{\alpha,2}, \dots, v_{\alpha,N}$ , and  $v_{\beta,1}, v_{\beta,2}, \dots, v_{\beta,N}$ , (28) takes the form:

$$\omega_{v,n} = \frac{v_{\alpha,n}v_{\beta,n-1} + v_{\beta,n}v_{\alpha,n-1}}{v_{\alpha,n}^2 + v_{\beta,n}^2}, \quad n \in \{2, \dots, N\}. \quad (29)$$

A complementary view interprets the phasor trajectory as a smooth planar curve parameterized by time. Let  $\mathbf{v} = v_\alpha \mathbf{e}_\alpha + v_\beta \mathbf{e}_\beta$  denote the real-imaginary projection of  $\bar{v}$  in the plane  $\mathcal{P}_{\alpha\beta} \in \mathbb{R}^2$  embedded in the ambient space  $\mathbb{R}^3$ , and let  $|\bar{v}| = |\mathbf{v}|$ . Its time derivative,  $\mathbf{v}'$ , can be decomposed orthogonally into its radial and tangential components [10]:

$$\mathbf{v}' = \rho_v \mathbf{v} + \boldsymbol{\omega}_v \times \mathbf{v}, \quad (30)$$

where  $\boldsymbol{\omega}_v = \omega_v \mathbf{e}_\gamma$  is an angular-velocity vector perpendicular to the plane  $\mathcal{P}_{\alpha\beta}$  and with magnitude  $\omega_v = |\boldsymbol{\omega}_v|$ . The first term describes instantaneous expansion or contraction of the trajectory (magnitude change), while the second represents rotational motion on the complex plane (phase evolution).

## REFERENCES

- [1] L. Mandel, "Interpretation of Instantaneous Frequencies," *American Journal of Physics*, vol. 42, no. 10, pp. 840–846, 1974.
- [2] L. Cohen, *Time-frequency Analysis*. Electrical engineering signal processing, Prentice Hall PTR, 1995.
- [3] J. Gutiérrez-Florensa, Á. Ortega, L. Sigrist, and F. Milano, "Quasi steady-state frequency," *IEEE Transactions on Circuits and Systems I: Regular Papers*, pp. 1–13, 2025.
- [4] Z. Gao, M. Fritz, G. Spalink, R. B. Staszewski, and M. Babaie, "A digital pll-based phase modulator with non-uniform clock compensation and non-linearity predistortion," *IEEE Journal of Solid-State Circuits*, vol. 58, no. 9, pp. 2526–2542, 2023.
- [5] J. Song, A. Mingotti, J. Zhang, L. Peretto, and H. Wen, "Fast iterative-interpolated DFT phasor estimator considering out-of-band interference," *IEEE Transactions on Instrumentation and Measurement*, vol. 71, pp. 1–14, 2022.
- [6] X. Nie, "Detection of grid voltage fundamental and harmonic components using Kalman filter based on dynamic tracking model," *IEEE Transactions on Industrial Electronics*, vol. 67, no. 2, pp. 1191–1200, 2020.
- [7] S. Giarnetti, F. Leccese, and M. Caciotta, "Non recursive multi-harmonic least squares fitting for grid frequency estimation," *Measurement*, vol. 66, pp. 229–237, 2015.
- [8] F. Wilches-Bernal, J. Wold, and W. H. Balliet, "A method for correcting frequency estimates for synthetic inertia control," *IEEE Access*, vol. 8, pp. 229141–229151, 2020.
- [9] F. Milano, "Complex frequency," *IEEE Transactions on Power Systems*, vol. 37, no. 2, pp. 1230–1240, 2022.
- [10] F. Milano, "A geometrical interpretation of frequency," *IEEE Transactions on Power Systems*, vol. 37, no. 1, pp. 816–819, 2022.
- [11] A. Alshawabkeh *et al.*, "Instantaneous frequency estimation in unbalanced systems using affine differential geometry," *IEEE Transactions on Circuits and Systems*, 2025.
- [12] F. Milano, G. Tzounas, I. Dassios, and T. Kérç, "Applications of the Frenet Frame to electric circuits," *IEEE Transactions on Circuits and Systems I: Regular Papers*, 2022.
- [13] J. Kaiser, "On a simple algorithm to calculate the 'energy' of a signal," in *Conference on Acoustics, Speech, and Signal Processing*, 1990.
- [14] P. Maragos and J. Kaiser, "On amplitude and frequency demodulation using energy operators," *IEEE Transactions on Signal Processing*, 1993.
- [15] A. Boudraa and F. Salzenstein, "Teager–kaiser energy methods for signal and image analysis: A review," *Digital Signal Processing*, vol. 78, 2018.
- [16] N. Shokouhi and J. Hansen, "TKEO for overlapped speech detection," *IEEE Transactions on Audio Speech and Language Processing*, 2017.
- [17] Y. Qin, "Multicomponent AM–FM demodulation based on energy separation and adaptive filtering," *Mechanical Systems and Signal Processing*, 2013.
- [18] I. Kamwa, K. Pradhan, and G. Joós, "Robust detection and analysis of power system oscillations using the teager-kaiser energy operator," *IEEE Transactions on Power Systems*, 2011.
- [19] IEEE Power & Energy Society and Power System Relaying and Control Committee, "Measuring relays and protection equipment – part 118-1: Synchrophasor for power systems – measurements," 2018.
- [20] P. Maragos, "Energy separation in signal modulations with application to speech analysis," *IEEE Transactions on Signal Processing*, 1993.
- [21] A. Derviškadić, G. Frigo, and M. Paolone, "Beyond phasors: Modeling of power system signals using the Hilbert transform," *IEEE Trans. Power Syst.*, vol. 35, no. 4, pp. 2971–2980, 2020.
- [22] J. Cexus and A. Boudraa, "Link between cross-Wigner distribution and cross-Teager energy operator," *Electronics Letters*, vol. 40, pp. 778–780, June 2004.
- [23] R. Hamila, J. Astola, A. Cheikh, M. Gabbouj, and M. Renfors, "Teager energy and the ambiguity function," *IEEE Transactions on Signal Processing*, vol. 47, pp. 260–262, Jan. 1999.
- [24] F. Milano, G. Tzounas, I. Dassios, and T. Kérç, "Applications of the frenet frame to electric circuits," *IEEE Transactions on Circuits and Systems I: Regular Papers*, vol. 69, no. 4, pp. 1668–1680, 2022.
- [25] F. Milano, "Equivalence between geometric frequency and lagrange derivative," *IEEE Transactions on Circuits and Systems I: Regular Papers*, vol. 72, pp. 4800–4809, 2024.
- [26] U. Frisch and B. Villone, "Cauchy's almost forgotten Lagrangian formulation of the Euler equation for 3D incompressible flow," *The European Physical Journal H*, vol. 39, no. 3, pp. 325–351, 2014.
- [27] F. Milano, G. Tzounas, I. Dassios, A. Murad, and T. Kérç, "Using differential geometry to revisit the paradoxes of the instantaneous frequency," *IEEE Open Access Journal of Power and Energy*, 2022.